



All-digital self-adaptive PVTA variation aware clock generation system for DFS

Jordi Pérez-Puigdemont, Antonio Calomarde and Francesc Moll
Dept. of electronic engineering, Univ. Politècnica de Catalunya, Barcelona, Spain
`jordi.perez-puigdemont@upc.edu`

February 23, 2015

Abstract

An all-digital self-adaptive clock generation system capable of adapt the clock frequency to compensate the effects of PVTA variations on the IC propagation delay and satisfy an externally set propagation length condition is presented. The design uses time-to-digital converters (TDCs) to measure the propagation length and a variable length ring oscillator (VLRO) to synthesize the clock signal. The VLRO naturally adapts its frequency to the PVTA variations suffered by its logic gates while the TDCs are used to track these variations across the chip and modify the VLRO length in order to adapt the clock frequency to them. The system measurements, for a 45nm FPGA, show that it adapts the VLRO length, and therefore the clock frequency, to satisfy the propagation length condition. Measurements also prove the system capabilities to act as a dynamic frequency scaling clock source since the propagation length condition value act as a frequency selection input and a strong linear relation between the input value and the resultant clock period is present.

1 Introduction

As transistor technology scales down the effects of process, voltage, temperature and ageing (PVTA) variations impact substantially on the integrated circuit (IC) performance, reliability and power consumption [1]. The rise in the transistor character-

istics uncertainty added to the rising complexity of the ICs leads to an increment of the effort needed to determine the main circuit parameters, such as the maximum operation frequency or supply voltage, that result in the desired IC yield. This effort increment is translated finally as more design cost and time. Until now this problem has been treated by adding extra margins to the IC parameters [2], e. g. lowering the clock frequency or rising the supply voltage, but now this margins may undermine the technology scaling gains [3].

In the recent years, to tackle the variability issue, researchers have proposed to adapt the clock frequency to the PVTA variations suffered by the IC. Some propose to detect timing in the datapath and to then correct them and/or adapt IC performance [4] but this technique implies a high architectural complexity. Other authors propose to use PVTA or delay sensors to adapt the clock frequency [5] which results in a slow responding system. In the same line others propose to use sensors to detect fast PVTA variations to stop the clock until the perturbation ends [4] but, if the variation lasts, the system could be stopped for a long time. We propose a closed loop adaptive system based on a variable length ring oscillator (VLRO) as clock source, which naturally adapts its frequency to dynamic or static PVTA variations, and time-to-digital converters (TDCs) as propagation delay sensors, more precisely as logic propagation length sensors, used to tune the length of the VLRO to ensure the adaptation condition: the TDCs worst output

should be equal to the input setpoint value [6]. By this way the proposed system can adapt continuously the clock frequency to PVT variations which can be homogeneous or heterogeneous along the die as well as operate as a dynamic frequency scaling system by changing the input setpoint value.

The article is organized as follows: in section 2 we show in a detailed way the proposed design for the adaptive system. In section 3, we discuss the field programmable gate array (FPGA) implementation of the system. In section 4 we present the measurements of the adaptive system implementation on a FPGA analysing its responses to homogeneous and heterogeneous static delay variations. Finally conclusions are drawn in section 5.

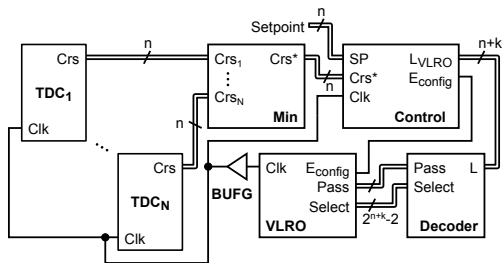


Figure 1: Scheme of the self-adaptive clock generation system.

2 System overview

The operation of an adaptive system can be explained very roughly as three step process that consists in, firstly, sensing a physical magnitude. Secondly comparing the sensing output with the desired objective. And, finally, perform the needed actions to minimize the difference between the measured magnitude and the objective. These processes are performed continuously in real time, either in sequence or simultaneously.

The proposed system is based on three different blocks that perform the adaptive process sequentially: a time-to-digital converter (TDC), a control block and a variable length ring oscillator (VLRO). First the TDCs sense the propagation length, it is

how deep a transition can travel through the logic path during one clock cycle, at different parts of the die. This logic depth is directly related with the clock period and inversely related with the logic gates propagation delay. After that the control block compares the worst of the TDC readings with the objective value, or setpoint, and decides the new VLRO length (which has to be decoded as the VLRO control vectors) that minimizes the adaptation error. And finally the VLRO is the circuit that synthesises the clock signal with the desired period, which has to be distributed to the whole die through the clock tree. Fig. 1 shows the self-adaptive clock generation system scheme.

The different adaptive system components will be discussed in detail in the next subsections: Sec. 2.1 for the TDC, Sec 2.2 for the control block and Sec. 2.3 for the VLRO.

2.1 Time-to-digital converter

The TDC used in the adaptive system is a circuit that outputs the number of stages in a delay line traversed by a positive transition within one clock period [7]. The TDC sensor schematic is depicted in Fig. 2. It is made of N TDC stages, each one has a delay stage made of k logic gates and a register that captures the state of the delay stage output to the Tap stage output. Also there is a offset delay, made of m logic gates. Varying m and k we can bias the output and the resolution of the sensor. Our system TDC also has a finite state machine (FSM) that is used to control its operation: injecting a rising pulse into the delay line, enabling the capture registers in the next clock cycle and waiting a given number of cycles until the process start again. The FSM is needed to synchronize all the TDCs scattered along the die between them and with the control block and the VLRO. For this reason all the FSM share the same reset signal and produce the same output signals. Finally the TDC is completed whit a binary encoder that simply outputs the number of stages traversed by the injected transition during one clock cycle.

Local PVT variations affect the delay of each TDC in the circuit. Each TDC output will therefore be determined by the local PVT conditions, as well

as by the common clock period. This behaviour can be observed in Fig. 3 where the measured output of a TDC sensor, implemented in a Xilinx Spartan(R)-3E (XC3S500E-4FG320C), is depicted. In this TDC the offset delay is made of 16 look up tables (LUTs) while each delay stage consist in 8 cascaded LUTs. The propagation delay is varied by modifying the FPGA core supply voltage: high voltage supply implies less propagation delay.

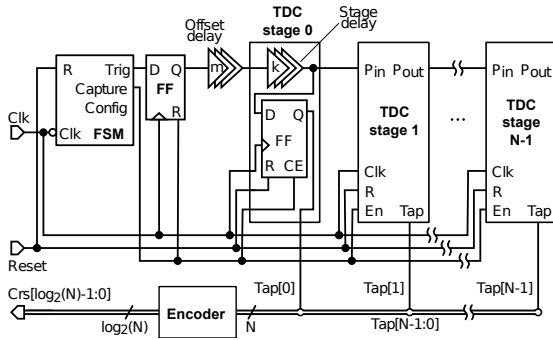


Figure 2: Time-to-digital converter (TDC) schematic. The purpose of the TDC sensor is to determine the number of delay stages crossed by a rising edge during one single period.

2.2 Control block

The control block is the circuit in charge of selecting the adequate length of the VLRO given the worst TDC output and the setpoint values. Its schematic can be viewed in Fig. 4. The control block calculates the adaptive error (Err in Fig. 4) as the difference between the setpoint value (SP) and the number of stages crossed (Crs^*). If we have more than one sensor the Crs^* value is the minimum of all the TDC outputs which represents the worst case. Then the error value is added to the last length of the VLRO (L_{prev}) in order to obtain the new VLRO length (L_{VLRO}). After calculating the L_{VLRO} value it has to be decoded as the VLRO configuration vectors $Pass$ and $Select$.

The operation of the control block is also governed by an instance of the same FSM used in the TDC sensor. It enables the registers that keep the value of

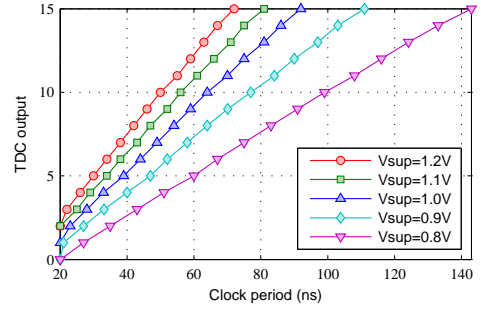


Figure 3: Output of a TDC sensor implemented on a Xilinx Spartan 3E FPGA for different clock period and different propagation delays induced by reducing the FPGA core voltage.

the setpoint and the last VLRO length at the same time when the registers of the TDC sensors capture the delay line state. A given number of clock periods after this, during one clock cycle, the FSM enables through the E_{config} signal the VLRO control registers. This waiting period gives enough time to the signal to travel the adaptive system worst path: from the Tap registers output in the TDCs (Fig. 2) to the VLRO control registers. By this way this path operates as a multi-cycle path.

2.3 Variable length ring oscillator

A VLRO acting as the clock generator has been chosen because it naturally adapts its oscillating frequency to the PVT variations suffered by its logic gates. Therefore, the VLRO will automatically adapt the clock period to the spatially homogeneously de-

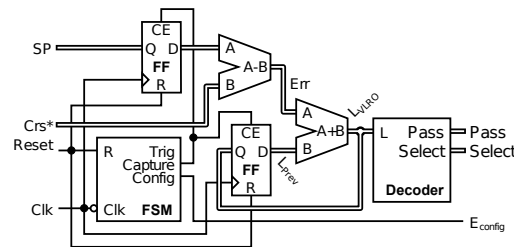


Figure 4: Adaptive system control block schematic.

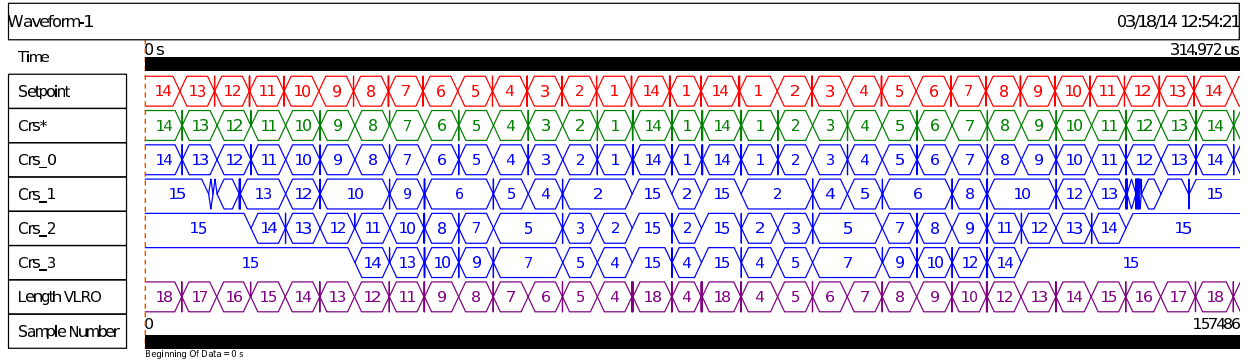


Figure 5: System internal signals, during a whole setpoint pattern, under the induced propagation delay static spatial variations. These signals have been measured with a logic analyzer.

lay variations, this is the variations that affect all the die in the same way statically or dynamically.

The VLRO used in the adaptive system is a fully-digital glitch-free VLRO [8]. It is important to stress that the registers that keep the value of the **Pass** and **Pass** control vectors are directly triggered by the clock output of the VLRO before it is injected in the global clock distribution tree. This will result in the presence of two shifted clocks with the same period: the VLRO local clock, only used by the VLRO registers, and the global clock, used by the rest of the adaptive system and the other registers in the die. This clock diversity is addressed using the **EConfig** enable signal for the VLRO control registers.

3 FPGA implementation

The system is implemented on a Xilinx Spartan-6(R) FPGA (XC6LX16-CS324). The adaptive system uses 4 TDC sensors. The setpoint and the number of TDC crossed stages are 4 bit width signals. This leads to a TDC delay line of 15 stages plus the offset stage. To study the system adaptation to static spatial variations the length of the offset and delay stages is different for every TDC in order to emulate the propagation delay variability across the chip. To analyse the produced clock response to different delay scenarios the propagation delay of the TDC stages are varied in the same way on all the TDCs. By this way we

are able to observe how the clock period is adapted to the sensors suffered delay.

The VLRO length use a 5 bit width signal letting to a VLRO with 32 stages each one made of one LUT. The FSM used in the TDCs and the control block waits for 5 clock periods after the **Capture** signal is enabled before setting to high the **Config** signal.

The VLRO block instances have been placed manually in order to assure a proper performance of the oscillator while we have led the software tools to place and route the TDC blocks, as well as the rest of the system blocks.

4 Experimental measurements

The measurements of the adaptive system are focused on the system operation and analysis of the clock signal and its period as well as on the system ability to adapt the clock period to a dynamically changing objective specifications. To do so we change the setpoint value every $10\mu\text{s}$ starting at 14 and decreasing it by one until it reaches 1, at this point the signal is changed to 14, to 1, again to 14 and finally returns to 1. After this the signal is increased by one until it reaches 14 and the cycle starts again. We deliberately avoid 15 an 0 setpoints values, so that these unused setpoints act as boundaries to the VLRO length set by the adaptive system.

In Fig. 5 the system signals measured with a logic

analyser are depicted, showing the system adaptation to the induced static spatial delay variation. This variation is emulated by design setting different offset and delay stage lengths for each TDC: for TDC_0 , 16 LUTs and 8 LUTs; for TDC_1 14 LUTs 7 LUTs; for the TDC_2 12 LUTs and 6 LUTs; and for the TDC_3 10 LUTs and 5 LUTs.

In Fig. 5 the different TDCs outputs (Crs_i) are shown, being TDC_0 the slowest one. For this reason, the Crs^* value corresponds to Crs_0 , and the adaptive system changes the VLRO length such that Crs^* achieves the setpoint value. Also one can observe in Fig. 5 that, in some cases, the same setpoint condition is satisfied by two different VLRO lengths (e. g. when the setpoint is equal to 7).

In Fig. 6 depicts the system signals during a setpoint change from 1 to 14 showing how the VLRO length is varied until the worst TDC output satisfies the setpoint condition.

To analyse how the clock period varies as function of the propagation length sensed by the TDCs and the setpoint value. The setpoint value is varied dynamically following the described pattern in above. Three propagation delay scenarios are emulated by setting the different lengths for the TDCs offset and delay stages. the longer the stages the bigger the propagation delay.

In Fig. 7 the clock signal period for the three described configurations along with the setpoint value are depicted. The figure clearly shows the correlation between the clock period and the setpoint value

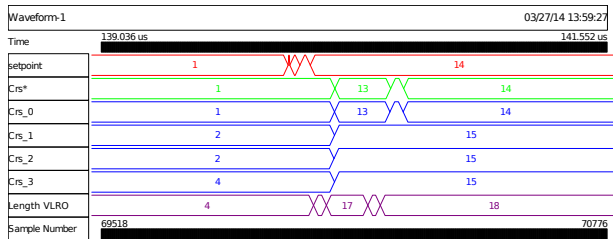


Figure 6: System internal signals under the induced propagation delay static spatial variations showing in detail how the system adapts the VLRO length, and hence the clock period, to an abrupt setpoint change.

which is the expected behaviour. Another expected result is also confirmed by the depicted measurements in Fig. 7: given the same setpoint values, the clock with the smallest period is produced by the configuration which induces less propagation delay to the TDCs (stage = 8 LUTs and offset = 16 LUTs). While the largest clock period is produced by the slowest TDC configuration (stage = 10 LUTs and offset = 20 LUTs). And the other configuration (stage = 9 LUTs and offset = 18 LUTs) always produces a clock signal with a period between two previously commented configurations.

In Fig. 7 is also depicted a metastability of the clock signal period. For the fastest sensor configuration (stage = 8 LUTs and offset = 16 LUTs) when the setpoint is equal to 3 the clock period changes between two values. This adaptive system response is caused because the system can not generate a clock signal that exactly satisfies the setpoint value, the worst TDC output oscillates between two values above and below the setpoint. This metastability is related with the relative difference between the propagation delay of a TDC stage with the period difference when the VLRO length is modified by one unit. This metastability can be suppressed by implementing a control block with some no-adaptation margins or designing it capable of identifying it.

To study more quantitatively the generated clock

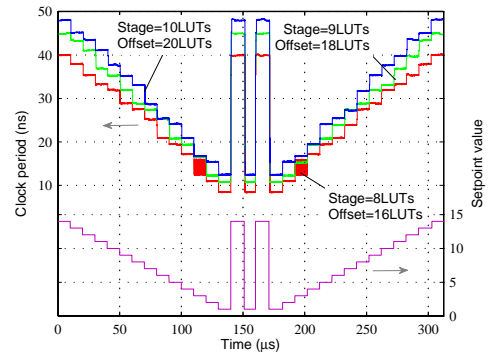


Figure 7: Setpoint value and clock period value for the three different induced propagation delay configurations over time.

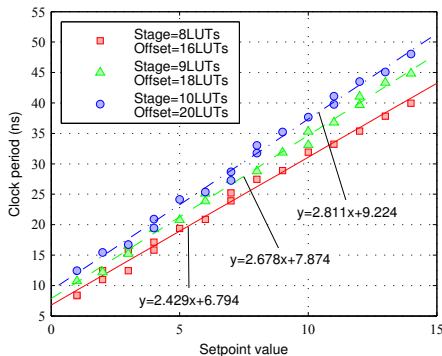


Figure 8: Clock period principal components for three different delay configurations as function of the setpoint value.

period the most frequent period values are plot in Fig. 8 for every delay configuration. The data show that, for some setpoints, the system produce two clock signal periods. This can be explained with the period metastability and the dual VLRO dual length setpoint condition fulfilment previously mentioned in the current article. The period follow, as function of the setpoint value, a linear relation for the three delay configurations. The period data and the derived linear equations confirm the behaviour pointed in Fig. 7: for sensor experiencing more propagation delay the clock period produced is bigger than the produced for sensors with less propagation delay.

5 Conclusions

In this article we proposed an all-digital self-adaptive clock generation system that is capable of adapting the clock period to spatially inhomogeneous PVTA variations. The self-adaptive systems is built using only digital blocks, even the clock synthesis circuit, which is a previously proposed VLRO oscillator. The adaptive system all-digital nature makes it easily portable between different technologies. The analysis of the internal signals show that the system autonomously adapt the length of the oscillator to satisfy the setpoint condition.

Since the setpoint can be set by an external sig-

nal and the produced clock period shows a linear response to the setpoint value the system can be used to provide dynamic frequency scaling capabilities as shown by the generated clock measurements. The existence of a setpoint input can be also used to integrated the proposed adaptive system within a datapath with timing error detection capabilities. The error detection system could determine, every given amount of time, the minimum setpoint value that operate the datapath without timing errors and the system will maintain it until the next error check. This integration would bring an IC with a clocking system that determines its maximum operation frequency and modifies it to allocate the delay variations induced by PVTA.

Acknowledgment

This work has been partially funded by the Spanish MINECO and ERDF (TEC2013-45638-C3-R).

References

- [1] K. Bowman, S. Duvall, and J. Meindl, "Impact of die-to-die and within-die parameter fluctuations on the maximum clock frequency distribution for gigascale integration," *IEEE Journal of Solid-State Circuits*, vol. 37, no. 2, pp. 183–190, 2002.
- [2] K. A. Bowman, S. G. Duvall, and J. D. Meindl, "Impact of die-to-die and within-die parameter fluctuations on the maximum clock frequency distribution for gigascale integration," *IEEE Journal of Solid State Circuits*, vol. 37, no. 2, pp. 183–190, 2002.
- [3] X. Wang, A. Brown, N. Idris, S. Markov, G. Roy, and A. Asenov, "Statistical threshold-voltage variability in scaled decananometer bulk HKMG mosfets: A full-scale 3-D simulation scaling study," *Electron Devices, IEEE Transactions on*, vol. 58, no. 8, pp. 2293–2301, 2011.
- [4] K. Bowman, J. Tschanz, S. Lu, P. Aseron, M. Khellah, A. Raychowdhury, B. Geuskens,

- C. Tokunaga, C. Wilkerson, T. Karnik, and V. De, "A 45 nm resilient microprocessor core for dynamic variation tolerance," *Solid-State Circuits, IEEE Journal of*, vol. 46, no. 1, pp. 194–208, Jan 2011.
- [5] C. R. Lefurgy, A. J. Drake, M. S. Floyd, M. S. Allen-Ware, B. Brock, J. A. Tierno, and J. B. Carter, "Active management of timing guardband to save energy in power7," in *Proceedings of the 44th Annual IEEE/ACM International Symposium on Microarchitecture*, ser. MICRO-44. New York, NY, USA: ACM, 2011, pp. 1–11.
- [6] J. Pérez-Puigdemont, A. Calomarde, and F. Moll, "Variation tolerant self-adaptive clock generation architecture based on a ring oscillator," in *SOC Conference (SOCC), 2012 IEEE International*, 2012, pp. 387–392.
- [7] A. Drake, R. Senger, H. Singh, G. Carpenter, and N. James, "Dynamic measurement of critical-path timing," in *Integrated Circuit Design and Technology and Tutorial, 2008. ICICDT 2008. IEEE International Conference on*, june 2008, pp. 249–252.
- [8] J. Perez-Puigdemont, F. Moll, and A. Calomarde, "All-digital simple clock synthesis through a glitch-free variable-length ring oscillator," *Circuits and Systems II: Express Briefs, IEEE Transactions on*, vol. 61, no. 2, pp. 90–94, Feb 2014.